Computers & Geosciences 130 (2019) 84–93

Contents lists available at ScienceDirect

Computers and Geosciences

journal homepage: www.elsevier.com/locate/cageo

Research paper

Mineral grains recognition using computer vision and machine learning

Julien Maitre *, Kévin Bouchard, L. Paul Bédard

Université du Québec à Chicoutimi, 555 boulevard de l'Université, Chicoutimi G7H2B1, Canada

ARTICLE INFO

Keywords:
Segmentation
Features
Machine learning
Ore
Sand grain
Recognition
Classification
Image processing

ABSTRACT

Identifying and counting individual mineral grains composing sand is an important component of many studies in environment, engineering, mineral exploration, ore processing and the foundation of geometallurgy. Typically, silt (32–128 μm) and sand (128–1000 μm) sized grains will be characterized under an optical microscope or a scanning electron microscope. In both cases, it is a tedious and costly process. Therefore, in this paper, we introduce an original computational approach in order to automate mineral grains recognition from numerical images obtained with a simple optical microscope. To the best of our knowledge, it is the first time that the current computer vision based on machine learning algorithms is tested for the automated recognition of such mineral grains. In more details, this work uses the simple linear iterative clustering segmentation to generate superpixels and many of them allow isolating sand grains, which is not possible with classical segmentation methods. Also, the approach has been tested using convolutional neural networks (CNNs). However, CNNs did not give as good results as the superpixels method. The superpixels are also exploited to extract features related to a sand grain. These image characteristics form the raw dataset. Prior to proceed with the classification, a data cleaning stage is necessary to get a usable dataset for machine learning algorithms. In addition, we present a comparison of performances of several algorithms. The overall obtained results are approximately 90% and demonstrate the concept of mineral recognition from a sample of sand grains provided by a numerical image.

1. Introduction

Identification or counting of minerals grains in sediments or sands is a critical task in many scientific endeavors. In environmental science, some minerals can release toxic elements such as arsenic (arsenopyrite; AsFeS) or lead (galena; PbS) (Hudson-Edwards, 2003). In some engineering projects using sand as a building material, some minerals in the sand can cause major problems in mortars (Lawrence et al., 2005). In mineral exploration geology, the abundance of minerals such as gold (Au) or chalcopyrite ($CuFeS_2$) in sediments or milled rock can indicate the proximity of a gold or copper mineral deposit (Averill, 2001). This technique is used on a vast scale by the diamond exploration industry, searching for grains of distinctive minerals such as chromium-bearing pyrope or diopside, minerals that are present with diamonds in kimberlite. It is at the base of controlling ore beneficiation efficiency in mining operation, where valuable minerals have to be concentrated from milled rocks (Wills and Finch, 2015). However, visual identification of minerals and the accurate estimation of their proportion is a lengthy, complex and an error prone task that has to be performed by highly trained personnel. Only the sheer amount of grains or particles to characterize (typically in the order of 200 000 to be statistically representative) render the operation tedious and time consuming. Two approaches are typically used to identify and characterize minerals grains in sediments or milled rocks: visual sorting with optical microscopy and automated Scanning Electron Microscopy (SEM) (Gottlieb et al., 2000; Sutherland and Gottlieb, 1991). Techniques such as chemical analysis and X-ray diffraction of sands or milled rocks will not provide a real mineral count. In the case of optical microscopy a highly qualified mineralogist will identify each individual mineral grain in a Petri dish at a typical rate of 60 grains per minute. It is a tedious work that needs lot of attention where any minute distraction can ruin a day's work. Also, it provides grain percentage instead of area percentage (Nie and Peng, 2014). The main drawbacks of the optical approach are the fatigue of highly qualified personnel leading to misidentification of minerals due to their lack of distinctive features and their small size. Alternatively, the SEM produces images of a mineral grains sample by scanning the surface with a focused beam of high-energy electrons to generate a variety of signals. Those signals are produced by electron-sample interaction and provide information such as the grain surface characteristics by secondary electrons (SE), its atomic density by backscattered electrons (BSE) and/or the chemical composition (from characteristic peaks in the X-ray spectrum). Mineral

* Corresponding author.
E-mail address: julien.maitre1@uqac.ca (J. Maitre).

https://doi.org/10.1016/j.cageo.2019.05.009
Received 4 February 2019; Received in revised form 13 May 2019; Accepted 21 May 2019
Available online 23 May 2019

grains are then segmented from the BSE or SE image, and an X-ray spectrum is acquired on each particle. Depending on the sophistication of the software used for analysis, X-ray spectrum can be deconvoluted into a chemical analysis and assigned to a mineral species (Grant et al., 2018). However, this technology has two major drawbacks, which are the price of the SEM (500 000 US$ to 2 M US$ depending on added options) and the long processing time for a single sample (1–5 h). These two cons translate into elevated cost and machine availability. For example, the fastest machine currently available can analyze a maximum of 40 000 grains per hour. Since approximately 200 000 grains is required to obtain acceptable statistical representativeness, the complete analysis requires approximately 5 h and cost 1000 US$ to process. Mineral exploration applications are particularly demanding due to the large size of samples to be scanned, and the large number of samples involved. In fact, the task is at the limit to be handled by current SEM technique. Minerals such as those indicating the presence of diamond hosting rock (kimberlite), such as chromium pyrope and chromium diopside, are visually distinctive, but not very chemically distinctive. And a single grain in millions of grains can be considered significant. Finding new mineral deposits is a difficult task because, among other reasons, most deposits are covered with vegetation or overburden, sediments from erosion such as glacial till. In glaciated terrains such as the Canadian Shield, glaciers have eroded mineral deposits and transported their characteristic minerals over a large area (Averill, 2001). These eroded sediments can be used as a proxy in exploration geology. Among those minerals eroded from a deposit, some will be diagnostic of the mineralization. The higher density minerals (above 3.3 g/cm^3; named heavy minerals in exploration) include the most characteristic minerals of deposits (named indicator minerals) such as gold and sulfides of copper, zinc, arsenic etc. For example, a large number of gold grains found in heavy mineral concentrates within a glacial till sample suggests proximity to a gold deposit (Shelp and Nichol, 1987).

Considering that in both aforementioned approaches (visual sorting and electron microscopy), identification of mineral grains is done sequentially, grain by grain. However, the present goal is to use images of a group of grains made with a relatively inexpensive tool, the optical microscope, where all grains can be characterized simultaneously from a single image. In this context, only few researchers have proposed computational methods based on cluster analysis to identify minerals (Baklanova and Shvets, 2014) using optical images. Indeed, with the recent emergence of the machine learning approach, computer science coupled to an optical microscope might become an interesting alternative to the SEM. Nevertheless, the current works in the literature deal only with the mineralogy. It focuses on detailed description of mineral grains such as the color (optical spectrum) to compute grain size and abundance.

The work proposed in this paper aims at demonstrating that computer vision coupled with data science and machine learning allow to perform mineral recognition. Indeed, an RGB image is acquired representing the sample of sand grains. Then, the same sample is scanned with an automated SEM programmed in order to generate a mineral map used as ground truth for the proposed approach. However, those two images representing the dataset are still unfeasible for mineral recognition. Thus, we had to implement a sophisticated methodology lying on segmentation, feature extraction and data cleaning in order to make the dataset acceptable. Finally, the mineral recognition was tested using three popular non-parametric classification methods, namely classification and regression trees (CART), the k-Nearest Neighbor (k-NN) and the random forest. Also, the convolutional neural network (CNN) approach was used as a baseline to assess the performance of our approach.

The first contribution presented in this study is the implementation of a sophisticated methodology for the creation of an acceptable dataset. Also, it is the first time that such a dataset is created for mineral recognition based on traditional machine learning algorithms. Due to the sand grains distribution on the sample and their characteristics, traditional segmentation techniques, such as edge-based segmentation, do not perform properly. Thus, we had to implement an original approach which is the superpixel segmentation. The second contribution is the extraction of new mathematical features on each sand grains of the sample. Indeed, it is the first time that mineral recognition based on machine learning is done. Thus, any mathematical sand grain features exist in the literature. The third contribution is the use of a machine learning algorithm in order to clean the dataset. In point of fact, an important amount of data is mislabeled due to random and large displacements of sand grains between the RGB image and the ground truth provided by the SEM. These displacements do not allow applying alignment algorithms, which are also very time consuming. Thus, it is very important to clean data in order to make acceptable the dataset for machine learning algorithms. The fourth and last contribution denotes the failed of the CNN approach in the segmentation (with the purpose of mineral recognition). Indeed, using CNNs in the present study is not suitable due to the difference (alignment, missing mineral sand grains in the ground truth between the original image and the ground truth image.

To the best of our knowledge, it is the first time that such a research is proposed to classify individual mineral grains with the use of such image processing, and the results presented in this paper prove the concept that mineral grains can be properly recognized by traditional machine learning algorithms.

The paper is organized as follows: Section 2 presents a brief state of the art on the mineral recognition methods. Section 3 describes the proposed method to classify mineral grains in a mineral species. Section 4 introduces the evaluation conditions of the machine learning algorithms, and then presents and discusses results. Finally, Section 5 briefly draws conclusions and provides an overview of potential future works.

2. Related work

As mentioned in Section 1, only few different techniques exist that are capable to evaluate the mineral proportions of a mineral grain sample such as a sediment or a milled rock. Those methods can be divided into two distinct groups, which are traditional engineering devices (Jarosewich et al., 1979; Chalmers et al., 2012; Kim et al., 2000) and the use of computational method based on computer vision (Baklanova and Shvets, 2014).

2.1. Traditional devices

The first group represents the popular way to evaluate mineral abundance in sediments or milled rock, such as used in mineral exploration or ore dressing: visual sorting under an optical microscope (Jarosewich et al., 1979) and automated particle analyses with the use of a scanning electron microscopy (Chalmers et al., 2012).

Visual sorting under optical microscopes needs to be conducted manually by highly qualified personnel. The mineralogist uses transmitted and reflected light properties of minerals to identify them, aside of their shape and morphology. Then, the slight differences in colors, luster, surface texture and grain shape can be detected by an expert human eye to identify the mineral species. To evaluate quantitatively the mineral abundances, grain counting technique is needed, which remains inefficient since it is time consuming and exhausting (Minnis, 1984). Specialized techniques have been developed to differentiate between very specific minerals in a controlled environment such as hematite and magnetite for the iron ore industry (Iglesias et al., 2011). These techniques are limited to very specific applications to be useful for broader applications. Moreover, mineral grain samples are difficult to prepare as thin or polished sections in a properly representative manner to Sorby (1882), Hutchison et al. (1974) fully use their optical properties for petrographic work. Furthermore, mineral surfaces

are considered significant, reflecting their attrition through sediment transport which are significative for indicator minerals, which surface cannot be observed on polished sections.

Alternatively, mineral grain analysis can be performed with specially equipped automated SEM (Nie and Peng, 2014; Philander and Rozendaal, 2013; Sylvester, 2012) and variation on SEM technology such as QEMSCAN (FEI Company; Hillsboro, Oregon, USA), TIMA-X (TESCAN, Brno, Czech Republic) and MLA (Sylvester, 2012) techniques routinely used in ore dressing, metallurgical science, forensic science or dust control, and paleoclimatic research. The SEM platform uses a focused beam of electrons scanning the surface of the material to generate an image of the mineral grains spread on a sample holder in our case. Then, the electrons interact with atoms in the sample. These interactions provide information (wave, electrons…) that are acquired by sensors to determine the chemical composition of minerals. Depending on the model and manufacturer, the SEM can provide various types of information such as secondary electrons, reflected or back-scattered electrons, characteristic X-rays and light (cathodoluminescence), absorbed current and transmitted electrons. The result of the analysis is given by an image of the mineral grain sample and complete statistics with mineral chemical composition (leading to identification), grain size and proportion of each mineral. There are other instruments that can perform a quantitative analysis of mineral such as electron microprobe (Jarosewich et al., 1979) but it is more time consuming than the SEM. The SEM analyzes mineral grains sequentially (one at a time). So, for large number of grains the throughput is seriously limited considering that each analysis takes a fraction to a few seconds depending on analytical quality defined by the operator.

2.2. Computational approach

The use of computational approaches based on the computer vision and machine learning in order to recognize minerals in a particulate sample are new and only one paper covers this field of research (Baklanova and Shvets, 2014). They Baklanova and Shvets (2014) applied a cluster analysis for the recognition of mineral in rocks for the mining industry by using the K-means algorithm. Clustering techniques allow partitioning a set of data into categories according to their similarities computed by a distance measurement such as the Euclidean distance. The defined characteristics of minerals are colors and textures. Those features are extracted from a reflected light image taken by a stereoscopic binocular microscope. The image reflects the structural features of the mineral grains. A vector of features has been implemented for each pixel. The vector is composed of the three spectral components (red, green, blue), and the average, variance, minimum and maximum brightness of the neighborhood pixels. However, the method does not perform a real recognition due to the exploitation of an unsupervised machine learning algorithm. In their work (Baklanova and Shvets, 2014), the researchers do not compare the found clusters with labeled cluster belonging to a species of mineral. Actually, their work only differentiates rocks, not their minerals. Hence, the method has only petrographic applications.

2.3. Techniques for similar images classification

Since few years and with the improvement of computational unit performances, new image classification algorithms have emerged. The most popular type of algorithm is the CNN, which belongs to the deep learning domain. This category of algorithm allows identifying the content of images without any image processing. This particularity denotes the major advantage of this type of algorithm. Indeed, a CNN has layers of convolutional filter linked to an artificial neural network. Thus, thanks to the convolutional filters, any human intervention is necessary to extract features related to the content of the image. In other terms, the feature extraction is performed at the same time that the training stage of the algorithm. However, the major drawbacks are that the learning is time consuming on a standard computer (e.g., 48 h in the present study for 10 epochs), and a CNN model need a large number of images to be trained properly (although it exists techniques that help to increase the size of the dataset — Data Augmentation). The primary function of Data Augmentation techniques is to avoid overfitting (Wang and Perez, 2017). Finally, this algorithm needs an important number of parameters that have to be set by the user. Fortunately, it exists architectures of CNN such as the AlexNet, GoogleNet, VGGNet and some others (Long et al., 2015).

3. Proposed method

For the purpose of the project, mineral concentrates were those obtained for gold grain counting. For such, 10 kg of natural glacial sediment samples were collected in the field, and sieved to less than 1 mm. The material is then processed with a fluidized bed to obtain a “superconcentrate” of approximately 100 mg which is demonstrated to retain nearly all gold grains present in the initial sample. The superconcentrate, containing in the order of 2 million grains smaller than 50 μm, has been sprinkled on a glued carbon tape to provide the image with a black backdrop for examination. Numerical photographs are taken by an automated motorized binocular microscope (Zeiss Axio-Zoom) to create a photomosaic. This photomosaic of high-resolution RGB images represents the only material used to achieve the classification of grains in mineral categories. The sample used for developing the current method is composed of grains from approximately 27 different mineral species in diverse proportions.

Once RGB image is acquired, the sample is scanned with an automated SEM programmed for mineral analysis. A mosaic of high resolution BSE image is acquired, from which grains are segmented, analyzed for chemical composition, and classified as mineral species. A map of grains of minerals is then obtained, which is referenced to the aforementioned RGB mosaic. The mineral map is then be used as “ground truth” for computer vision. SEM acquisition of the mineral map required more than 12 h.

The work presented in this paper describes a first attempt to develop a method to recognize grains of minerals from a particulate material, such as a sediment, with the use of a computational approach relying on three completely different although complementary domains: computer vision, data science and machine learning. Thus, in order to carry out the mineral classification for each grain composing the sand, an image segmentation is applied to isolate mineral grains. Then, characteristics can be extracted from each isolated grain. Those characteristics represent discriminant information about the color, luster, relief and surface texture of the grains. The vector composed of features and labeled with a mineral species is called an instance. The mineral species represents a class (category in machine learning and “class” is not used to mean the mineralogical class) and some instances denote the dataset. Thereafter, a cleaning stage of the data is necessary due to the mislabeling of instances when compared to the mineral map obtained from SEM (“the ground truth”). To do so, outlier instances were excluded from each class. Once the dataset is acceptably clean to be exploited by the machine learning algorithms, the dataset was divided into two groups of examples. The first one represents 70% of the instances and it is used to train the algorithms. The second group was composed of 30% of the dataset and enables testing the performances of the algorithms.

In summary, the proposed method relies on four steps (Fig. 1). The first one is the data labeling. The second represents the feature extraction. The third denotes the post-processing of data including a cleaning data phase in order to train and evaluate the machine learning algorithms in the fourth step.

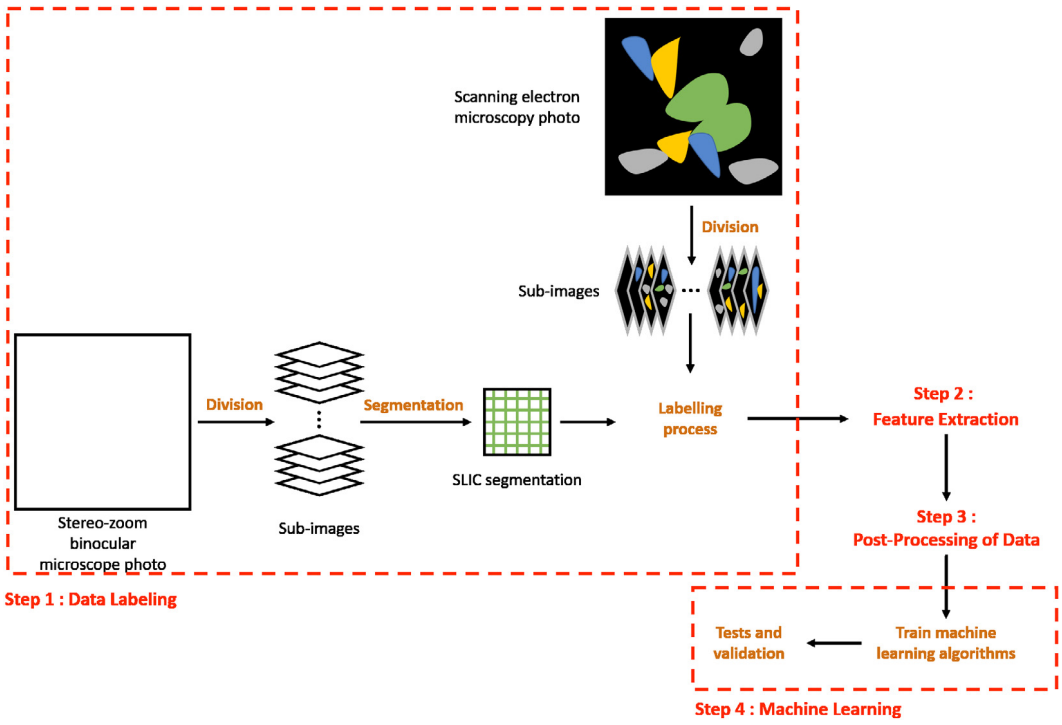

Fig. 1. Steps of the proposed method for the recognition of mineral grains from an RGB image of mineral grain sample.

3.1. Data labeling

The general purpose of this work is to exploit an RGB image representing a sample of mineral grains of different species (plagioclase, ilmenite, monazite, magnetite. etc.), which was taken with a motorized although conventional microscope. Images were taken with a 6 megapixels camera with a field of view of 2.5 x 2 mm. In order to cover the entire surface of the sample surface, a total of 238 field of view were required, allowing for 10% overlaps between adjacent field. Images were then stitched into a large mosaic using ImageJ application (Rasband, 1997). Therefore, a mosaic image of 34 674 x 33 720 pixels (~2 GBytes) is generated and used for computer vision. Fig. 2 shows photographs of sample: the photomosaic of the entire sample (Fig. 2a) and a detailed view showing individual mineral grains (Fig. 2b). Due to the large size of the original image, this picture was divided into 600 x 600 pixels sub-images, which represents a total number of 3192 images. Fig. 2b illustrates one of those.

To perform a mineral recognition, data from each mineral grain of images have to be labeled and extracted. The labeling process is carried out following a two-step process. The first one is the difficult task of segmenting sub-images. Indeed, considering the shapes of mineral grains, the color variations and the mutually touching grains, traditional methods of segmentation (e.g., edge-based segmentation) are ineffective into separating individual mineral grains. Additionally, the VGG-16 (Simonyan and Zisserman, 2014) was implemented for the segmentation of images. VGG-16 is a particular architecture (number of convolutional layer, size of the filter ...) of CNN. Despite a reasonable accuracy (~87%), it did not produce meaningful results due to the abundant amount of background pixels, the low number of images for the training step and the absence of texture information. It shall be mentioned that the major problem of using CNN for the segmentation in the current research is the difference (alignment, missing mineral sand grains in the ground truth) between the original images and the ground truth image.

In this context, superpixel segmentation is an excellent alternative way to separate mineral grain data (Li and Chen, 2015). Superpixel segmentation provides coherent regions of pixels in order to compute local features. The initial idea of this method described in Li and Chen (2015) is to over-segment an image decreasing at the same time the complexity of image processing tasks. The algorithm used is simple linear iterative clustering (SLIC) that produces a fast and a high quality segmentation (Achanta et al., 2012). This method performs a local clustering of pixels based on their color similarity and proximity in the sub-image. It uses five-dimensional space given by [labxy], where l, a and b values are the pixel color vector provided by the CIELAB color space and the x, y are the coordinates of the pixel. Also, to cluster pixels in the [labxy] space, we need a distance measure considering the desired number of approximately equally sized superpixel K. Also, the segmentation gives the coordinates in the [xy] plane of each superpixel. Additionally, we increased the contrast of the image in order to discriminate more easily the borders of sand grains. Fig. 4 shows a result of the SLIC segmentation on one sub-image.

The second step is to match each superpixel with the class labels of the original ground truth. The original ground truth is also an image of 34 674 x 33 720 pixels provided by the scanning electron microscopy (SEM), in which a mineral species (identification) has been assigned to each and every mineral grain based on its chemical signature. Also, we need to align the two images providing by optical microscopy and SEM respectively. To perform this, we located coordinates (pixels) of triangle vertices in the source image (optical microscopy image) and the coordinates of the corresponding triangle vertices in the destination image (SEM image). Then, an affine transform (2×3 matrix) is calculated from these pairs of pixels and applied to the destination image. Once the alignment has been performed, the original ground truth image is divided into 600 x 600 pixels sub-images in order to use the previous [xy] coordinates obtained from the segmentation. Provisional colors are then attributed to each pixel based on mineral species to obtain the ground truth image. Fig. 3b shows the ground truth sub-image corresponding to Fig. 3a. Each superpixel is then tagged with the class label according to the two predominant provisional colors.

As it can be seen by comparing Fig. 3a and b, these two sub-images do not perfectly superimpose. Random minute displacements of the particles were induced by the degassing of the glue holding grains by the vacuum pumping in the SEM. Consequently, the ground

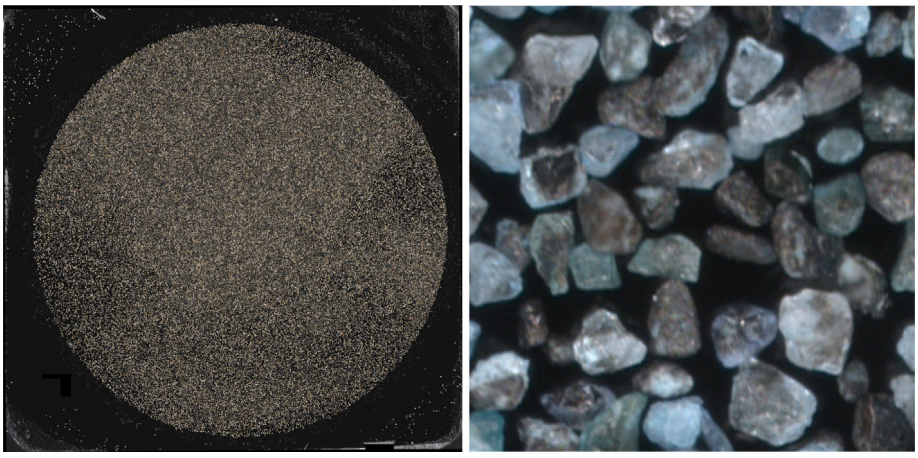

(a) (b)

Fig. 2. (a) The original photomosaic of sample surface (approximately 35 mm diameter); (b) RGB sub-image of 600 x 600 pixels as used for image segmentation.

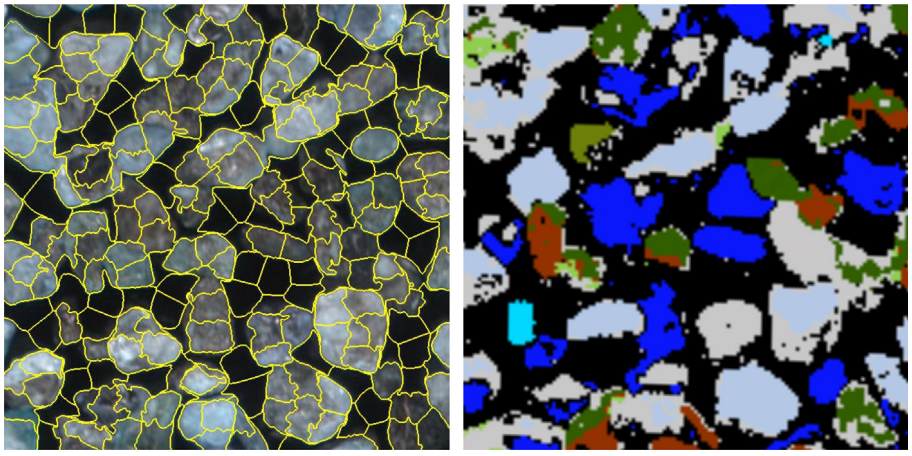

(a) (b)

Fig. 3. (a) Result of the SLIC segmentation on one sub-image; (b) The ground truth sub-image provided by the SEM where minerals are identified in provisional colors. (For interpretation of the references to color in this figure legend, the reader is referred to the web version of this article.)

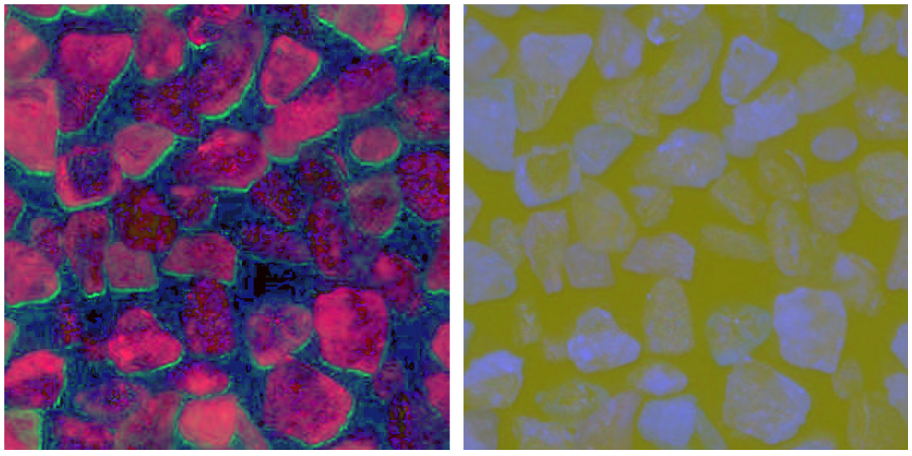

(a) (b)

Fig. 4. (a) HSV color space representation of one sub-image; (b) Lab color space representation of one sub-image.

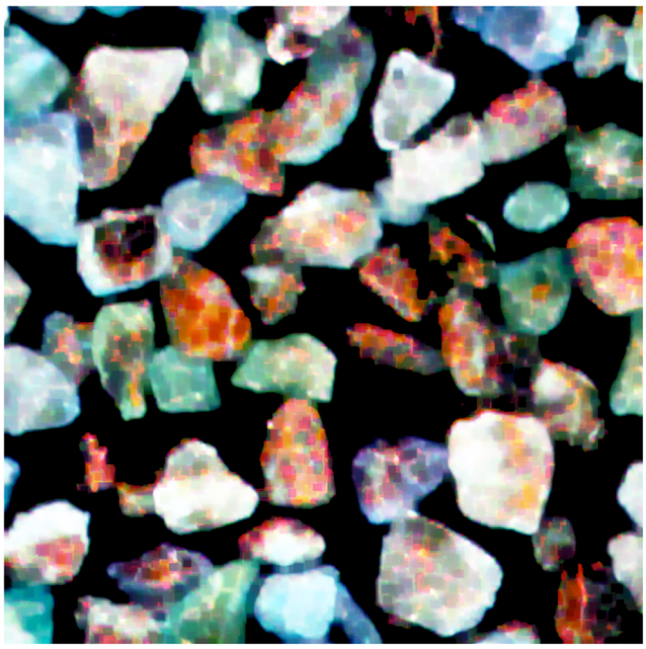

Fig. 5. Improvement of colors differentiation for one sub-image. (For interpretation of the references to color in this figure legend, the reader is referred to the web version of this article.)

truth provided by the SEM does not perfectly match the optical image. Furthermore, some mineral grains are not properly identified, and some grains are composed of more than one mineral. Post-processing of data has been required after the feature extraction. Nevertheless, the quality of the classification is undoubtedly affected by the poor quality of the ground truth. Procedures to avoid these issues are currently being tested.

3.2. Feature extraction

Feature extraction from superpixels is necessary for proper labeling. Features are a quantification of the parameters that allow describing a phenomenon with a single value. In other words, features are values that represent a discriminant information allowing to differentiate objects (e.g., mineral grains).

In the course of visual sorting, minerals are recognized by their color, luminance, luster and surface texture properties (Baklanova and Shvets, 2014). Thus, different color spaces are necessary to properly quantify these properties. The first one is the RGB color space of an original sub-image as illustrated in Fig. 2. Then, each sub-image undergoes a series of representation transformation. RGB is converted into HSV (Hue, Saturation, Value) color space (Agoston, 2005). HSV is an alternative representation of the RGB color space allowing to separate the image intensity from color information. Fig. 4 illustrates the HSV color space for a sub-image. The image is also converted into Lab color space (Connolly and Fleiss, 1997) which considers perceptual uniformity for small color distances. Fig. 4 represents the Lab color space for a sub-image. These transformations improve the original image by allowing discriminating subtleties in mineral grain colors. Fig. 5 shows the color improvement. Different steps are necessary to obtain this last sub-image. First, simple thresholding is applied to provide a mask discerning mineral grains from the background (in black). Secondly, the brightness of the sub-image is increased (+50). Thirdly, a new image is produced by applying the mask on the image with a better brightness. Fourthly, saturation is enhanced (+50). Fifthly, contrast is improved by equalizing RBG histograms. Finally, a morphological transformation is performed in order to close small holes inside the foreground of the heavy mineral sample (Gonzalez et al., 2004). The objective of this last step is to uniformize the color of mineral grains with a dilation followed by an erosion operation.

Each superpixel of each sub-image representation is used to extract a set of features. Features are the mean, the standard deviation, the skewness and the kurtosis coefficient for each channel of each sub-image representation. For a superpixel j on the channel i, we have:

$$mean_{channel_{ij}} = \frac{\sum_{k=1}^{N} x_{channel_{ik}}}{N}, \tag{1}$$

$$std_{channel_{ij}} = \sqrt{\frac{\sum_{k=1}^{N}(x_{channel_{ik}} - mean_{channel_{ij}})^2}{N-1}}, \tag{2}$$

$$skewness_{channel_{ij}} = \frac{\frac{1}{N}\sum_{k=1}^{N}(x_{channel_{ik}} - mean_{channel_{ij}})^3}{std^3{}_{channel_{ij}}}, \tag{3}$$

and

$$kurtosis_{channel_{ij}} = \frac{\frac{1}{N}\sum_{k=1}^{N}(x_{channel_{ik}} - mean_{channel_{ij}})^4}{std^4{}_{channel_{ij}}}, \tag{4}$$

where $x_{channel_{ik}}$ is the value of the pixel k in the color channel $channel_i$, and N denotes the total number of pixels for one superpixel. However, those features are not sufficient for a recognition.

As cited previously, the luminance is one property allowing humans to identify mineral species. The luminance average, called degree of luminance, is computed for each superpixel with Eq. (5) and considered as another feature.

$$DegreeOf\,Luminance = \frac{\sum_{k=1}^{N}(0.22 \times x_{red_k} + 0.71 \times x_{green_k} + 0.07 \times x_{blue_k})}{N}, \tag{5}$$

Also, according to the fact that different variations of colors can have the same average value, the RGB histograms could serve to differentiate colors more efficiently than the mean (Huang et al., 2010). A histogram provides a graphical representation of the distribution of colors in an image. In other words, it produces a discretization of the

colors in the image into a number of bins (fixed list of color ranges), and determines the number of image pixels in each bin. In this work, the RGB histograms for each superpixel are computed. Fig. 6 illustrates the R, G and B histograms for the corresponding superpixel.

From those histograms, the feature extracted are the coordinates of the first and second maximum peak in each histogram. The coordinates represent the number of pixels divided by the total number of pixels and the corresponding bin.

Coordinates of the first and second maximum peak, or peak intensity (ratio between the number of pixels to total number of pixels) and color intensity (quantile), are extracted as features for each superpixels. Finally, a textural coefficient is computed for each superpixel, which represents the number of white pixels divided by the total number of pixels in a superpixel. This last feature is obtained by applying a canny edge detector to each sub-image.

3.3. Data post-processing

Due to random displacements between the SEM ground truth and the optical image, the instances (attributes and labels) dataset had to be cleaned. To perform this, a first description about the dataset is necessary. The dataset has a total of 786 655 instances. Among all these instances, there are 287 classes. The majority of those cannot be used due to the small number of occurrences. Furthermore, the imbalance of instances among categories affects the training phase of machine learning algorithms and their performances during the classification test (Yen and Lee, 2006). For example, we have a total of 2 instances for the "Actinolite, Plagioclase" class and 16 566 occurrences for the "Plagioclase, None" category. In addition, the classification algorithm used to process SEM data yields a category named "Unknown", in which particle with an ambiguous composition was not allocated with a mineral name. The classification fails when the chemical composition of a mineral exceed the specified tolerance in distance in the Euclidian hyperspace due to impurities, mixed signal or spectral deconvolution issues. Consequently, all instances labeled as "Unknown" were excluded from learning to avoid contaminating the other classes. Thus, we decided to exclude all instances with the word "Unknown" in their label because the sand grains normally belong to a known mineral and to avoid contaminating the other classes. Also, particle identified as "Quartz" are overwhelmingly dominant (47 570 instances), but plagued with various color issues. Quartz is typically colorless and transparent. However, it may be stained by iron oxide coating, tinted by internal structural damages, or be loaded with submicroscopic inclusions that alter its apparent color. Being transparent and bi-refracting, light traversing the grains tends to disperse as in a prism into "rainbows". Furthermore, due to transparency, quartz particle may reflect the color light form neighboring grains. Consequently, instances labeled as "Quartz" were eliminated from the dataset. Finally, to prove the computer vision and machine learning concept, classes that are not pure were excluded. For example, instances labeled as "Plagioclase, None" were considered as pure and were preserved, while instances labeled as "Plagioclase, Magnetite" were not considered as pure and disregarded. Once post-processed, 546 444 instances were retained, labeled into 9 classes. Among these instances, the "Background" class account for 468 431 instances.

Due to the random displacement of the particles between the optical image and the SEM ground truth, misclassification of some instances during the labeling process is unavoidable. Outlier data by using the isolation forest algorithm (Liu et al., 2008). Outlier data or anomalies with different features from normal instances were excluded. To identify them, the algorithm builds an ensemble of trees allowing to isolate every single instance. Isolated data close to the root of the tree structure are considered as anomalies, while normal instances are isolated in a leaf of the tree.

The deployment of this algorithm needs as argument the fraction of outlier data. A human analysis permitted to determine that 60% of the data samples are mislabeled. Therefore, for each class, 60% of the instances are excluded.

Finally, in order to correct the imbalance of instances between classes, the dataset that can be exploited for a first minerals recognition is presented in Table 1.

Table 1
Dataset exploited for mineral recognition.

Classes	Number of instances
Plagioclase	5000
Augite	820
Background	5000
Hypersthene	2471
Ilmenite	1148
Magnetite	5000
Microcline	1099
Titanite	976
Hornblende	5000

3.4. Machine learning algorithms

3.4.1. Classification and regression trees

The Classification and Regression Trees (CART) is a supervised machine learning algorithm proposed by Breiman et al. in 1984 (Kelleher et al., 2015). It represents a binary decision tree constructed from the training dataset in a recursive way. Its advantages are the high performance and the ease of implementation due to the tree architecture. This algorithm has no parameter settings and can deal with numerical values and categorical attributes of the dataset. The final decision tree is generated in two steps, which are the construction of the maximum tree and the choice of the right size tree (reduction of the maximum tree). In other words, the classification tree is constructed by using a divide and conquer approach.

3.4.2. k-nearest neighbors

The k-Nearest Neighbors (k-NN) (Kelleher et al., 2015) is the simplest classification algorithms. k-NN is defined as a non-parametric lazy learning algorithm. In other terms, any model is computed. However, the algorithm needs all training dataset for the classification process of a new instance. This results into costly processing time when the number of occurrences is very large. This method relies on determining the k nearest neighbors among all the training dataset of the new observation x by computing distances between x and each training data. Then, the new instance gets the label (class) y of the predominant category among the k nearest neighbors. The user selects the number k of nearest neighbors and the type of distance (Euclidean distance, Chebyshev distance, etc.).

3.4.3. Random forest

A Random Forest (RF) is a supervised machine learning algorithm proposed by Breiman in 2001 (Breiman, 2001). It presents the advantages to be simple, flexible and efficient. Indeed, a RF is a combination of decision trees, where each tree is constructed by using a random vector of values (sampled independently with the same distribution). Thus, the algorithm can be modeled by a "forest" of random trees. The final classification is given by a majority vote between each decision of each tree. For such an algorithm, the user has to set parameters, which are the number of trees in the forest, the number of features to consider for the best split, and the measurement function to determine the quality of the split.

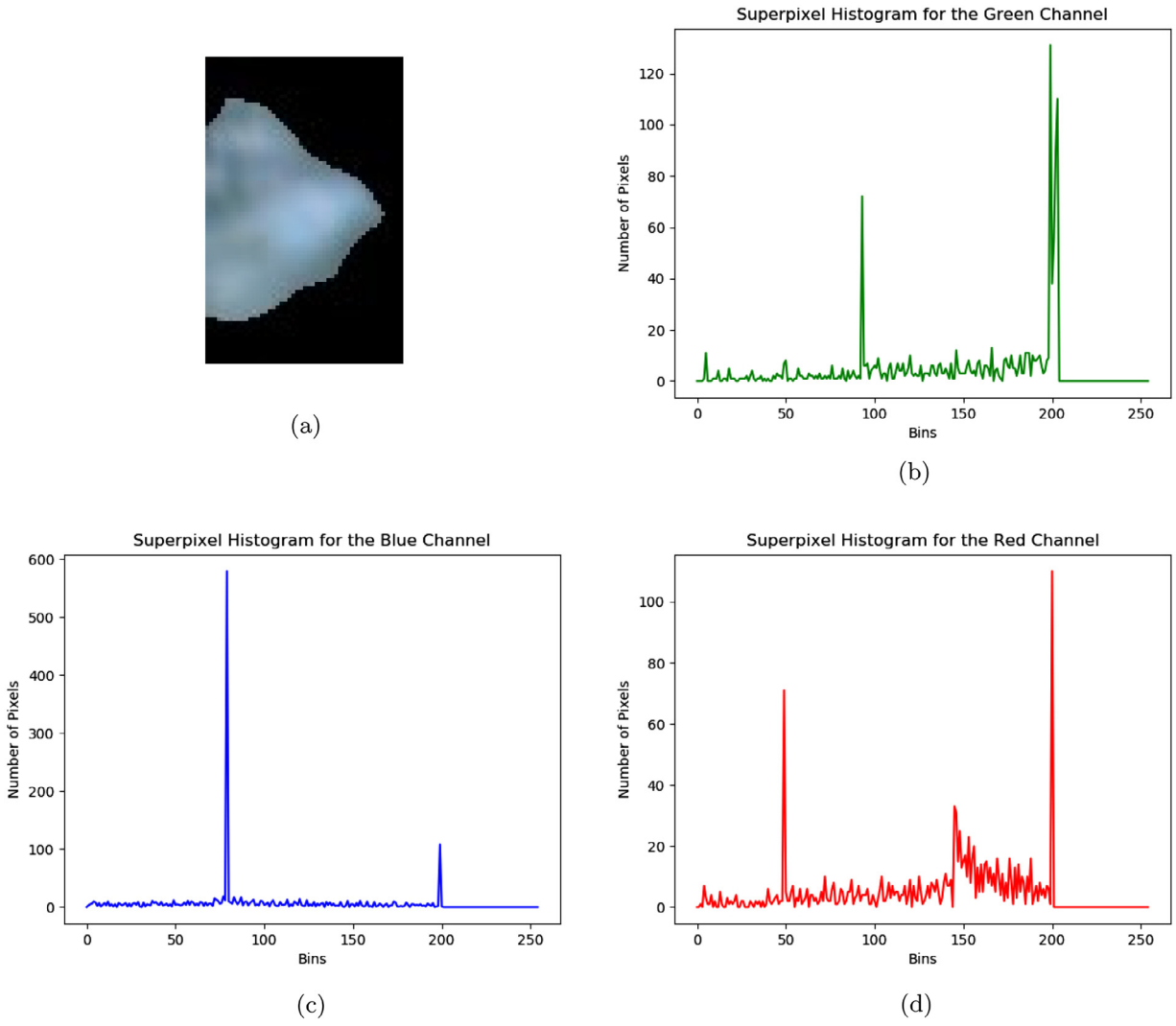

Fig. 6. (a) Superpixel given by the mineral grain in color; (b) Histogram of the green channel; (c) Histogram of the blue channel; (d) Histogram of the red channel.

4. Results and discussion

In this section, we present some results for the recognition of mineral grains from an image provided by a stereo-zoom binocular microscope. As described in Section 3, the dataset exploited for the classification had undergone a labeling, feature extraction and post-processing processes. Finally, the dataset is presented in Table 1.

In order to recognize minerals of sand grains by using the algorithms described in Section 3, a classical split of the dataset is applied. It allows generating a training and testing datasets. The ratio is 70–30. In other words, it means that 70% of instances serve to train the machine learning algorithms, and 30% of the dataset tests them.

Comparison of performances between these algorithms can be done by using well-known indicators such as the precision (P), recall (R), f1-score (F1-s) and the kappa statistics (Witten et al., 2016). The performances are expressed in a table containing the global performances of the classifier and the micro-performances per classes.

Tables 2–4 show that the random forest algorithm gives the best results for the mineral species classification. Indeed, the global accuracy is respectively +12% and +6% better than CART and k-NN algorithms.

As expected, classification performances of low abundances mineral species, based on a small number of instances, are significantly lower than the more abundant ones. The main reason is that the algorithms cannot be well trained for those classes compared to other mineral species with a high number of occurrences. Thus, the categories with a low number of instances are excluded from the dataset. Results using the five most abundant classes are provided in Tables 5 to 7.

Table 2
Classification results with CART.

CART				
Global Accuracy	0.66			
Global Kappa	0.60			
	P	R	F1-s	Support
Plagioclase	0.82	0.78	0.80	1500
Augite	0.24	0.27	0.25	246
Background	1	1	1	1500
Hypersthene	0.64	0.59	0.62	742
Ilmenite	0.28	0.30	0.29	345
Magnetite	0.58	0.59	0.58	1500
Microcline	0.17	0.19	0.18	330
Titanite	0.49	0.54	0.51	293
Hornblende	0.61	0.61	0.61	1500

An improvement of the mineral recognition by excluding less abundant species is indicated in Tables 5–7. Global accuracy for the best algorithm is improved at 89%. This represents promising outcomes and random forest algorithm is indicated for subsequent works. In addition, Tables 5–7 show really good performances of mineral recognition for the plagioclase.

Table 3
Classification results with k-NN.

k-NN				
Global Accuracy	0.72			
Global Kappa	0.67			
	P	R	F1-s	Support
Plagioclase	0.80	0.92	0.86	1500
Augite	0	0	0	246
Background	1	1	1	1500
Hypersthene	0.64	0.74	0.69	742
Ilmenite	0.18	0.01	0.01	345
Magnetite	0.58	0.77	0.66	1500
Microcline	0.17	0.01	0.01	330
Titanite	0.80	0.37	0.50	293
Hornblende	0.62	0.70	0.66	1500

Table 4
Classification results with RF.

RF				
Global Accuracy	0.82			
Global Kappa	0.73			
	P	R	F1-s	Support
Plagioclase	0.83	0.94	0.88	1500
Augite	1	0.02	0.04	246
Background	1	1	1	1500
Hypersthene	0.71	0.78	0.74	742
Ilmenite	0.66	0.18	0.28	345
Magnetite	0.65	0.82	0.73	1500
Microcline	0.43	0.03	0.05	330
Titanite	0.77	0.53	0.63	293
Hornblende	0.71	0.81	0.75	1500

Table 5
Classification results with CART on classes composed of a high number of instances.

CART				
Global Accuracy	0.83			
Global Kappa	0.78			
	P	R	F1-s	Support
Plagioclase	0.91	0.92	0.92	1500
Background	1	1	1	1500
Hypersthene	0.80	0.80	0.80	742
Magnetite	0.69	0.70	0.69	1500
Hornblende	0.73	0.71	0.72	1500

Table 6
Classification results with k-NN on classes composed of a high number of instances.

k-NN				
Global Accuracy	0.85			
Global Kappa	0.82			
	P	R	F1-s	Support
Plagioclase	0.94	0.92	0.93	1500
Background	1	1	1	1500
Hypersthene	0.82	0.87	0.84	742
Magnetite	0.72	0.78	0.75	1500
Hornblende	0.79	0.70	0.74	1500

The confusion matrix for the results of the Random Forest Algorithm on reduced number of class is provided in Table 8. The "Plagioclase, None" and "Background" categories are well discriminated, while the magnetite and hornblende classes can be confused one to the another.

5. Conclusion

The described computational approach to perform the mineral classification of mineral grains starting from an optical microscope image is considered new and innovative, with multiple scientific and industrial applications. The proposed solution relies on the image and

Table 7
Classification results with RF on classes composed of a high number of instances.

RF				
Global Accuracy	0.89			
Global Kappa	0.86			
	P	R	F1-s	Support
Plagioclase	0.96	0.94	0.95	1500
Background	1	1	1	1500
Hypersthene	0.83	0.87	0.85	742
Magnetite	0.78	0.83	0.80	1500
Hornblende	0.85	0.80	0.82	1500

Table 8
Confusion matrix of the classification with RF on classes composed of a high number of instances.

	Plagioclase	Background	Hypersthene	Magnetite	Hornblende
Plagioclase	1407	0	24	46	23
Background	0	1500	0	0	0
Hypersthene	25	0	645	55	17
Magnetite	21	0	63	1243	173
Hornblende	17	0	42	246	1195

data processing and machine learning algorithms that classifies vectors of mineral features with efficiency. Also, this research exploits the superpixel segmentation as an efficient alternative to traditional segmentation methods in order to isolate each mineral grain. To the best of our knowledge, it is the first time that such approach is used with success. It proves the concept that computer supported computer vision can be used to classify mineral species in particulate material, such as sand. Specific applications can be foreseen where the abundance of a specific mineral of commercial value can be estimated in a fast and dependable way within mineral processing plants, or where rare but specific mineral of interest can be spotted in sands in order to detect mineralized occurrences for the mineral exploration industry.

Results of this study demonstrate that the proposed approach is efficient at recognizing mineral species given that a sufficiently high number of instances is used for learning. In this particular experiment, the grains are from a single location. For larger application, a more diverse set of learning minerals should be used. Performances of classification algorithm can be in excess of 80%. Using Random Forest algorithm for learning leads to the best mineral reconnaissance rates with a global accuracy approximately equal to 90%. The gain in productivity can be quite high. First of all, in term of monetary investment as optical microscopes are less expensive than SEM and are much cheaper to maintain. Then, the time required to acquire the optical images are much faster than SEM or the time spent by a experienced person that identify each mineral grain.

The current work presents a solution to mineral species automated reconnaissance among particulate material such as a natural sand. Results are considered very promising. Nevertheless, improvement in the technique is still needed to render it more robust. Indeed, the sand used in this study come from the same region, which implies that the method presented in this article will not recognize correctly mineral sand coming from other regions in the world. Indeed, sand grains from other regions have mineralogical differences that could impact the quality of the classification. Thus, we need to integrate mineral sand grains of other regions into our model or to create a model for each region.. Among others, a solution might be to acquire images of the sample under different light sources, such as planar or circular polarized light or different wavelength such as near infrared or ultraviolet lights. More features would be extracted in order to better differentiate similar minerals species. The labeling process has to be improved to reduce the rate of mislabeling. Improvements might be achievable in regard of superpixels segmentation, or the quality of the extracted features.

6. Computer code availability

- Name of code : Mineral Grain Recognition
- Developpers : Julien Maitre
- Contact details : Université du Québec à Chicoutimi, 555 boulevard de l'Université, Chicoutimi G7H2B1, Canada; e-mail: julien.maitre1@uqac.ca
- Year first available : 2019
- Hardware required : Mineral Grain Recognition was run on a computer with 4 cores (2.4 GHz each) and 16 GB.
- Software required : Mineral Grain Recognition was interpreted with Pycharm IDE and needs scikit-learn, scikit-image, opencv and numpy packages
- Program language : the code is written in Python 3.6
- Program size : 184 kb
- Details on how to access the source code : the source files of the Mineral Grain Recognition can be downloaded from github : https://github.com/julienmaitre/Mineral-Recognition

CRediT authorship contribution statement

Julien Maitre: Conceptualization, Methodology, Investigation, Software, Writing - original draft, Writing - review & editing. **Kévin Bouchard:** Supervision, Writing - original draft. **L. Paul Bédard:** Funding acquisition, supervision, Writing - original draft, Writing - review & editing.

Acknowledgments

Alexandre Néron and Jonathan Tremblay are thanked for the help in providing optical and electronic image and data. Réjean Girard provided the original idea and shared some of his near infinite energy. Alexandre Néron is also thanked to have attracted LPB attention to machine learning. This study was funded by a Fonds de Recherche du Québec - Nature et Technologies (FRQ-NT) grant to L.P.B. with contributions from IOS Servives Géoscientifiques Inc (Projet de recherche orienté en partenariat; Grant number: 2015-MI-191750).

References

Achanta, R., Shaji, A., Smith, K., Lucchi, A., Fua, P., Süsstrunk, S., et al., 2012. SLIC Superpixels compared to state-of-the-art superpixel methods. IEEE Trans. Pattern Anal. Mach. Intell. 34 (11), 2274–2282. http://dx.doi.org/10.1109/TPAMI.2012.120.

Agoston, M., 2005. Computer Graphics and Geometric Modeling: Implementation and Algorithms. Springer, Berlin.

Averill, S.A., 2001. The application of heavy indicator mineralogy in mineral exploration with emphasis on base metal indicators in glaciated metamorphic and plutonic terrains. Geolog. Soc., London, Spec. Publ. 185 (1), 69–81. http://dx.doi.org/10.1144/GSL.SP.2001.185.01.04.

Baklanova, O., Shvets, O., 2014. Cluster analysis methods for recognition of mineral rocks in the mining industry. In: Image Processing Theory, Tools and Applications (IPTA), 2014 4th International Conference on. IEEE, pp. 1–5. http://dx.doi.org/10.1109/IPTA.2014.7001972.

Breiman, L., 2001. Random forests. Mach. Learn. 45 (1), 5–32. http://dx.doi.org/10.1023/A:1010933404324.

Chalmers, G.R., Bustin, R.M., Power, I.M., 2012. Characterization of gas shale pore systems by porosimetry, pycnometry, surface area, and field emission scanning electron microscopy/transmission electron microscopy image analyses: Examples from the barnett, woodford, haynesville, marcellus, and doig units. AAPG Bull. 96 (6), 1099–1119. http://dx.doi.org/10.1306/10171111052.

Connolly, C., Fleiss, T., 1997. A study of efficiency and accuracy in the transformation from rgb to cielab color space. IEEE Trans. Image Process. 6 (7), 1046–1048. http://dx.doi.org/10.1109/83.597279.

Gonzalez, R.C., Woods, R.E., Eddins, S.L., et al., 2004. Digital Image Processing Using MATLAB, vol. 624. Pearson-Prentice-Hall Upper Saddle River, New Jersey.

Gottlieb, P., Wilkie, G., Sutherland, D., Ho-Tun, E., Suthers, S., Perera, K., Jenkins, B., Spencer, S., Butcher, A., Rayner, J., 2000. Using quantitative electron microscopy for process mineralogy applications. Jom 52 (4), 24–25. http://dx.doi.org/10.1007/s11837-000-0126-9.

Grant, D., Goudie, D., Voisey, C., Shaffer, M., Sylvester, P., 2018. Discriminating hematite and magnetite via scanning electron microscope–mineral liberation analyzer in the- 200 mesh size fraction of iron ores. Appl. Earth Sci. 127 (1), 30–37. http://dx.doi.org/10.1080/03717453.2017.1422334.

Huang, Z.-C., Chan, P.P., Ng, W.W., Yeung, D.S., 2010. Content-based image retrieval using color moment and gabor texture feature. In: Machine Learning and Cybernetics (ICMLC), 2010 International Conference on, vol. 2. IEEE, pp. 719–724. http://dx.doi.org/10.1109/ICMLC.2010.5580566.

Hudson-Edwards, K., 2003. Sources, Mineralogy, Chemistry and Fate of Heavy Metal-Bearing Particles in Mining-Affected River Systems. De Gruyter, http://dx.doi.org/10.1180/0026461036720095.

Hutchison, C.S., et al., 1974. Laboratory Handbook of Petrographic Techniques. Wiley.

Iglesias, J.C.A., Gomes, O.d.F.M., Paciornik, S., 2011. Automatic recognition of hematite grains under polarized reflected light microscopy through image analysis. Miner. Eng. 24 (12), 1264–1270. http://dx.doi.org/10.1016/j.mineng.2011.04.015.

Jarosewich, E., Nelen, J.A., Norberg, J.A., 1979. Electron microprobe reference samples for mineral analyses. Smithson. Contrib. Earth Sci. 22, 68–72.

Kelleher, J.D., Mac Namee, B., D'Arcy, A., 2015. Fundamentals of Machine Learning for Predictive Data Analytics: Algorithms, Worked Examples, and Case Studies. MIT Press.

Kim, C.S., Brown Jr, G.E., Rytuba, J.J., 2000. Characterization and speciation of mercury-bearing mine wastes using x-ray absorption spectroscopy. Sci. Total Environ. 261 (1–3), 157–168. http://dx.doi.org/10.1016/S0048-9697(00)00640-9.

Lawrence, P., Cyr, M., Ringot, E., 2005. Mineral admixtures in mortars effect of type, amount and fineness of fine constituents on compressive strength. Cem. Concr. Res. 35 (6), 1092–1105. http://dx.doi.org/10.1016/j.cemconres.2004.07.004.

Li, Z., Chen, J., 2015. Superpixel segmentation using linear spectral clustering. In: Proceedings of the IEEE Conference on Computer Vision and Pattern Recognition, pp. 1356–1363.

Liu, F.T., Ting, K.M., Zhou, Z.-H., 2008. Isolation forest. In: 2008 Eighth IEEE International Conference on Data Mining. IEEE, pp. 413–422. http://dx.doi.org/10.1109/ICDM.2008.17.

Long, J., Shelhamer, E., Darrell, T., 2015. Fully convolutional networks for semantic segmentation. In: Proceedings of the IEEE Conference on Computer Vision and Pattern Recognition, pp. 3431–3440, http://dx.doi.org/10.1109/CVPR.2015.7298965.

Minnis, M.M., 1984. An automatic point-counting method for mineralogical assessment. AAPG Bull. 68 (6), 744–752.

Nie, J., Peng, W., 2014. Automated sem–eds heavy mineral analysis reveals no provenance shift between glacial loess and interglacial paleosol on the chinese loess plateau. Aeolian Res. 13, 71–75. http://dx.doi.org/10.1016/j.aeolia.2014.03.005.

Philander, C., Rozendaal, A., 2013. The application of a novel geometallurgical template model to characterise the namakwa sands heavy mineral deposit, west coast of south africa. Miner. Eng. 52, 82–94. http://dx.doi.org/10.1016/j.mineng.2013.04.011.

Rasband, W., 1997. Imagej software. Nat. Inst. Health: Bethesda, MD, USA 2012.

Shelp, G.S., Nichol, I., 1987. Distribution and dispersion of gold in glacial till associated with gold mineralization in the canadian shield. J. Geochem. Explor. 28 (1–3), 315–336. http://dx.doi.org/10.1016/0375-6742(87)90055-0.

Simonyan, K., Zisserman, A., 2014. Very deep convolutional networks for large-scale image recognition. arXiv preprint arXiv:1409.1556.

Sorby, H., 1882. Preparation of transparent sections of rocks and minerals. North. Microsc. 17 (101–106), 133–140.

Sutherland, D., Gottlieb, P., 1991. Application of automated quantitative mineralogy in mineral processing. Miner. Eng. 4 (7–11), 753–762. http://dx.doi.org/10.1016/0892-6875(91)90063-2.

Sylvester, P.J., 2012. Use of the mineral liberation analyzer (mla) for mineralogical studies of sediments and sedimentary rocks. Mineral. Assoc. Can. 1–16.

Wang, J., Perez, L., 2017. The effectiveness of data augmentation in image classification using deep learning. Convol. Neural Netw. Vis. Recog..

Wills, B.A., Finch, J., 2015. Wills' Mineral Processing Technology: an Introduction to the Practical Aspects of Ore Treatment and Mineral Recovery. Butterworth-Heinemann.

Witten, I.H., Frank, E., Hall, M.A., Pal, C.J., 2016. Data Mining: Practical Machine Learning Tools and Techniques. Morgan Kaufmann.

Yen, S.-J., Lee, Y.-S., 2006. Under-sampling approaches for improving prediction of the minority class in an imbalanced dataset. In: Intelligent Control and Automation. Springer, pp. 731–740. http://dx.doi.org/10.1007/978-3-540-37256-1_89.